Published in final edited form as:
Opt Express. 2006 May ; 14(10): 4280–4285.

Homodyne scanning holography

Joseph Rosen*
Department of Electrical and Computer Engineering, Ben-Gurion University of the Negev, P. O. Box 653 Beer-Sheva 84105, Israelrosen@ee.bgu.ac.il, http://www.ee.bgu.ac.il/~rosen

Guy Indebetouw*
Department of Physics, Virginia Polytechnic Institute and State University, Blacksburg, Virginia 24061 gindebet@vt.edu, http://www.phys.vt.edu/people/indebetouw.html

Gary Brooker
Department of Biology, Integrated Imaging Center, Johns Hopkins University, Montgomery County Campus 9605 Medical Center Drive, Rockville, MD 20850 gbrooker@jhu.edu, http://www.jhu.edu/iicmcc/

Abstract

We have developed a modified version of a scanning holography microscope in which the Fresnel Zone Plates (FZP) are created by a homodyne rather than a heterodyne interferometer. Therefore, during the scanning the projected pattern on the specimen is frozen rather than varied as previously. In each scanning period the system produces an on-axis Fresnel hologram. The twin image problem is solved by a linear combination of at least three holograms taken with three FZPs with different phase values.

1. Introduction

Fluorescence microscopy is widely used in many areas of biology. Digital holography [1] is a well established technique for three-dimensional (3D) imaging of micro structures. However, digital holograms are recorded by interfering two mutual coherent beams and therefore cannot be applied to the incoherent light which is the characteristic of the emitted light in a fluorescent microscope. Scanning holography [2-4], on the other hand, is the only method so far that has demonstrated the ability to produce a hologram of the fluorescent emission distributed in a 3D structure. However, scanning holography, in its previous form, has been recorded by a heterodyne interferometer in which the holographic information has been coded on a high carrier frequency. Such method suffers from several drawbacks. On one hand, trying to keep the scanning time as short as possible requires using carrier frequencies which are higher than the bandwidth limit of some, or all of the electronic devices in the system. On the other hand, working with a carrier frequency, that is lower than the system limitation, extends the scanning time far beyond the minimal time needed to capture the holographic information according to the sampling theorem. Long scanning times limit the system from recording dynamical scenes.

In this paper we combine the two holographic techniques scanning and digital holography to a single method of recording on-line Fresnel holograms of microscopic fluorescence samples after laser excitation. In this modified system, the hologram is recorded without temporal carrier frequency using homodyne interferometer. By doing this we offer an improved method of 3D imaging which can be applied to fluorescence microscopy. To the best of our knowledge,

*On sabbatical at Department of Biology, Integrated Imaging Center, Johns Hopkins University, Montgomery County Campus

it is first time that scanning holography is demonstrated by a homodyne rather than heterodyne interferometer.

2. Principles of homodyne scanning holography

In classic heterodyne scanning holography a pattern of Fresnel Zone Plates (FZP) scans the object and at each and every scanning position the light intensity is integrated by a detector. The overall process is a 2D convolution operation between the object and the FZP patterns. Our modified scanning holography is also a method of convolution by scanning the object with a set of frozen-in-time FZP patterns. The FZP is created by interference of two mutually coherent spherical waves. As shown in Fig. 1, the interference pattern is projected on the specimen, scans it in 2D, and the reflected light from the specimen is integrated on an area detector. Due to the line-by-line scanning by the FZP along the specimen, the one dimensional signal detected is composed of the entire lines of the convolution matrix between the object function and the FZP. In the computer, the detected signal is reorganized in the shape of a 2D matrix the values of which actually represent the Fresnel hologram of the specimen. The specimen we consider is 3D, and its 3D structure is stored in the hologram by the effect that during the convolution, the number of cycles of the FZP (its Fresnel number) contributed from a distant object point is slightly smaller than the number of cycles of the FZP contributed from closer object points.

As mentioned above the FZP is the intensity pattern of the interference between two spherical waves given by,

$$F(x,y,z)=Ap(x,y)\left\{1+\exp\left[\frac{i\pi}{\lambda(\gamma+z)}\left(x^2+y^2\right)+i\theta\right]+\exp\left[\frac{-i\pi}{\lambda(\gamma+z)}\left(x^2+y^2\right)-i\theta\right]\right\}, \quad (1)$$

where $p(x,y)$ is a disk function with the diameter D that indicates the limiting aperture on the projected FZP, A is a constant, θ is the phase difference between the two spherical waves and λ is the wavelength of the light source. The constant γ indicates that at a plane $z=0$ there is effectively interference between two spherical waves, one emerging from a point at $z=-\gamma$ and the other converging to a point at $z=\gamma$. This does not necessarily imply that these particular spherical waves are exclusively needed to create the FZP. For a 3D specimen $S(x,y,z)$ the convolution with the FZP of Eq. (1) is,

$$\begin{aligned} O(x,y;\gamma) &= S(x,y,z) * F(x,y,z) = \int S(x,y,z) * p(x,y)\,dz \\ &+ \int\int\int S(x',y',z')\,p(x-x',y-y')\exp\left\{\frac{i\pi\left[(x-x')^2+(y-y')^2\right]}{\lambda(\gamma+z')}+i\theta\right\}dx'dy'dz' \\ &+ \int\int\int S(x',y',z')\,p(x-x',y-y')\exp\left\{\frac{-i\pi\left[(x-x')^2+(y-y')^2\right]}{\lambda(\gamma+z')}-i\theta\right\}dx',dy',dz', \end{aligned} \quad (2)$$

where the asterisk denotes a 2D convolution. Note that $O(x,y;\gamma)$ is a 2D function which is different for different values of the parameter γ. This convolution result is similar to a conventional Fresnel on-axis digital hologram, and therefore, it suffers from the same problems. Specifically, $O^{th}(x,y;\gamma)$ of Eq. (2) contains three terms which represent the information on three images namely the 0 diffraction order, the virtual and the real images. Trying to reconstruct the image of the specimen directly from a hologram of the form of Eq. (2) would fail because of the disruption originated from two images out of the three. This difficulty is solved here with the same solution applied in an on-axis digital holography.

Explicitly, at least three holograms of the same specimen are recoded, where for each one of them a FZP with a different phase value is introduced. A linear combination of the three holograms cancels the two undesired terms and the remaining is a complex valued on-axis Fresnel hologram which contents only the information of the single desired image, either the virtual, or the real one, according to our choice. A possible linear combination of the three holograms to extract a single convolution between the object and one of the quadratic phase function of Eq. (2), is

$$O_F(x,y;\gamma) = O_1(x,y;\gamma)\left[\exp(\pm i\theta_3) - \exp(\pm i\theta_2)\right] + O_2(x,y;\gamma)\left[\exp(\pm i\theta_1) - \exp(\pm i\theta_3)\right] + O_3(x,y;\gamma)\left[\exp(\pm i\theta_2) - \exp(\pm i\theta_1)\right], \quad (3)$$

where $O_i(x,y;\gamma)$ is the ith recorded hologram of the form of Eq. (2) and θ_i is the phase value of the ith FZP used during the recording. The choice between the signs in the exponents of Eq.v (3) determines which image, virtual or real, is kept in the final hologram. If for instance the virtual image is kept, $O_F(x,y;\gamma)$ is the final complex valued hologram of the form,

$$O_F(x,y;\gamma) = \int S(x,y,z') * p(x,y) \exp\left[\frac{i\pi}{\lambda(\gamma+z')}\left(x^2+y^2\right)\right] dz'. \quad (4)$$

The function $O_F(x,y;\gamma)$ is the final hologram which contains the information of only one image - the 3D virtual image of the specimen in this case. Such image $S'(x,y,z)$ can be reconstructed from $O_F(x,y;\gamma)$ by calculating in the computer the inverse operation to Eq. (4), as follows,

$$S'(x,y,z) = O_F(x,y;\gamma) * \exp\left[\frac{-i\pi}{2\lambda z}\left(x^2+y^2\right)\right]. \quad (5)$$

The resolution properties of this imaging technique are determined by the properties of the FZP. More specifically the diameter D and the constant γ characterize the system resolution in a similar way to the effect of an imaging lens [5]. Suppose the image is a single infinitesimal point at z=0, then $O_F(x,y;\gamma)$ gets the shape of a quadratic phase function limited by a finite aperture. The reconstructed point image has a transverse diameter of $1.22\lambda\gamma/D$, which defines the transverse resolution, and an axial length of $2\lambda\gamma^2/D^2$ which defines the axial resolution. Note also that the width of the FZP's last ring along its perimeter is about $\lambda\gamma/D$, and therefore the size of the specimen's smallest distinguishable detail is approximately equal to the width of this ring.

3. Experimental results

To demonstrate the proposed technique, the setup shown in fig.1 was built on a standard wide-field fluorescence microscope (ZEISS, Axiovert S100). The specimen was a slide with several pollen grains [Carolina Biological Slide No. 30-4264(B690)] positioned at different distances from the microscope objective. The microscope objective was a Zeiss infinity corrected Fluar 20×, NA=0.75. The slide was illuminated by the FZP created by the interferometer. A DPSS-532 laser beam (λ=532nm) was split in two beams with beam expanders consisting each of a microscope objective and a 12-cm focal-length achromat as a collimating lens. One of the beams passed through an electro-optic phase modulator (New Focus 4002) driven by three (or more) constant voltage values which induce three (or more) phase difference values between

the interfering beams. Note that unlike previous studies [2-4] there is no frequency difference between the two interfering waves since this time we record a hologram with a homodyne interferometer. The two waves were combined by the beam splitter to create an interference pattern in the space of the specimen. The pattern was then reduced in size and projected through the objective onto the specimen. The sample was scanned in a 2D raster with an *X*-*Y* piezo stage (Physik Instrument P-527). The data were collected by a GageScope CS1602 acquisition system, and data manipulation was performed by programs written in MATLAB.

The three recorded holograms of the specimen taken with phase difference values of $\theta_{1,2,3}=0$, $\pi/2$, and π are shown in Fig. 2, respectively. In this figures it clearly appears that the dominant term is the low frequency term [the first in Eq. (2)], and therefore without mixing the three holograms in the linear combination that eliminates the low frequency along with the twin image term, there is no possibility to recover the desired image with a reasonable quality. These three holograms are substituted into Eq. (3) and yield a complex valued hologram shown in Fig. 3. This time the grating lines are clearly revealed in the phase pattern.

The computer reconstruction of two pollen grains along the z axis is shown in the movie of Fig. 4. As can be seen in this movie different parts of the pollen grains are in focus at different transverse planes.

4. Conclusions

We have presented and verified experimentally a modified version of a scanning holography system. This setup has some advantages over the previous designs but there are problems that should be solved in the future. The main technical difficulty is that during the serial scanning of each hologram there is a slight shift in the phase value of each FZP. This phase shift introduces some error and uncertainty in the measured phase value of each hologram. In future work, we intend more closely temporally correlate each point in each of the three holograms so as to minimize this phase error. Nevertheless, the proposed system is more immune from noise and it operates faster than previous scanning holography systems.

Acknowledgments

The authors thank Maria DeBernardi and Brian Storrie for valuable comments during this research. Part of the computer programming was done by Wenwei Zhong. This research is supported by the National Science Foundation grant DBI-0420382. J. Rosen's research is supported in part by the Israel Science Foundation grant 119/03. G. Indebetouw's research is supported in part by the National Institute of Health grant 5R21 RR18440.

References and links

1. Yamaguchi I, Zhang T. “Phase-shifting digital holography,”. Opt. Lett 1997;22:1268–1269. [PubMed: 18185816]
2. Schilling BW, Poon T-C, Indebetouw G, Storrie B, Shinoda K, Suzuki Y, Wu MH. “Three-dimensional holographic fluorescence microscopy”. Opt. Lett 1997;22:1506–1508. [PubMed: 18188283]
3. Indebetouw G, El Maghnouji A, Foster R. “Scanning holographic microscopy with transverse resolution exceeding the Rayleigh limit and extended depth of focus,”. J. Opt. Soc. Am. A 2005;22:892–898.
4. Indebetouw G, Klysubun P, Kim T, Poon T-C. “Imaging properties of scanning holographic microscopy,”. J. Opt. Soc. Am. A 2000;17:380–390.
5. Goodman, JW. Introduction to Fourier Optics. Vol. 2nd ed. McGraw-Hill, New York: 1996. p. 126-165.

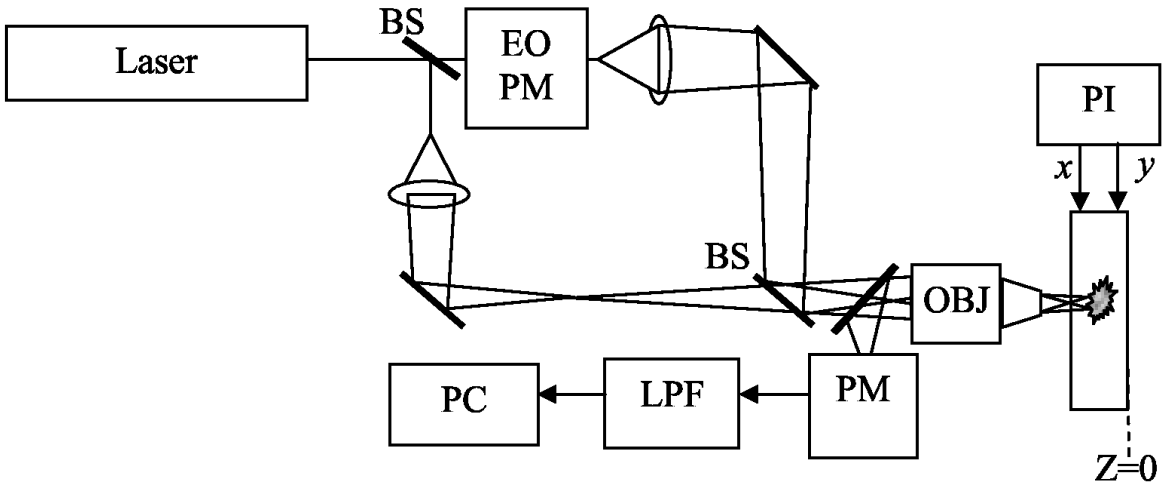

Fig. 1.

Optical setup: EOPM, electro-optic phase modulator introducing a phase difference between the two beams; BS, beam splitter; PI, piezo XY stage, OBJ, objective; PM, photomultiplier tube detector; LPF, lowpass filter; PC, personal computer.

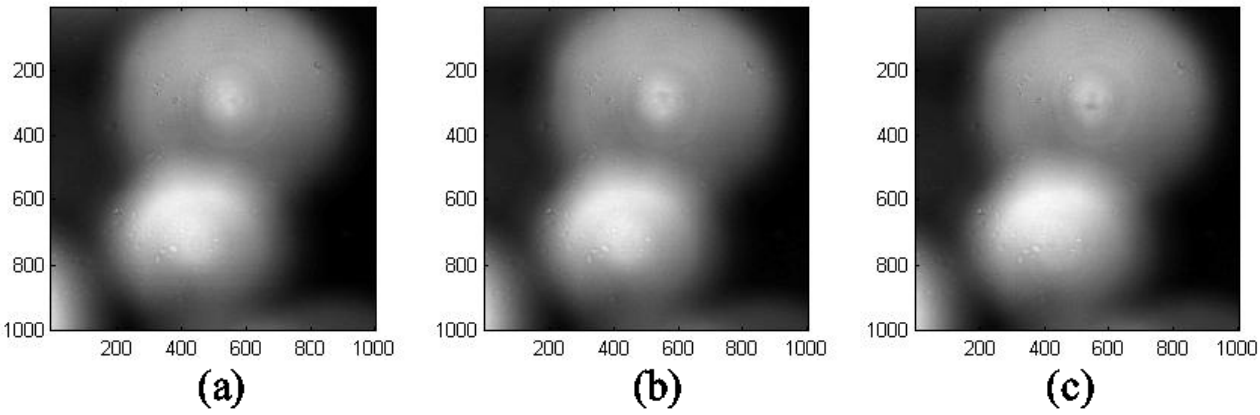

Fig. 2.
Three recorded holograms with phase difference between the two interferometers arms of (a) 0 (b) $\pi/2$ and (c) π.

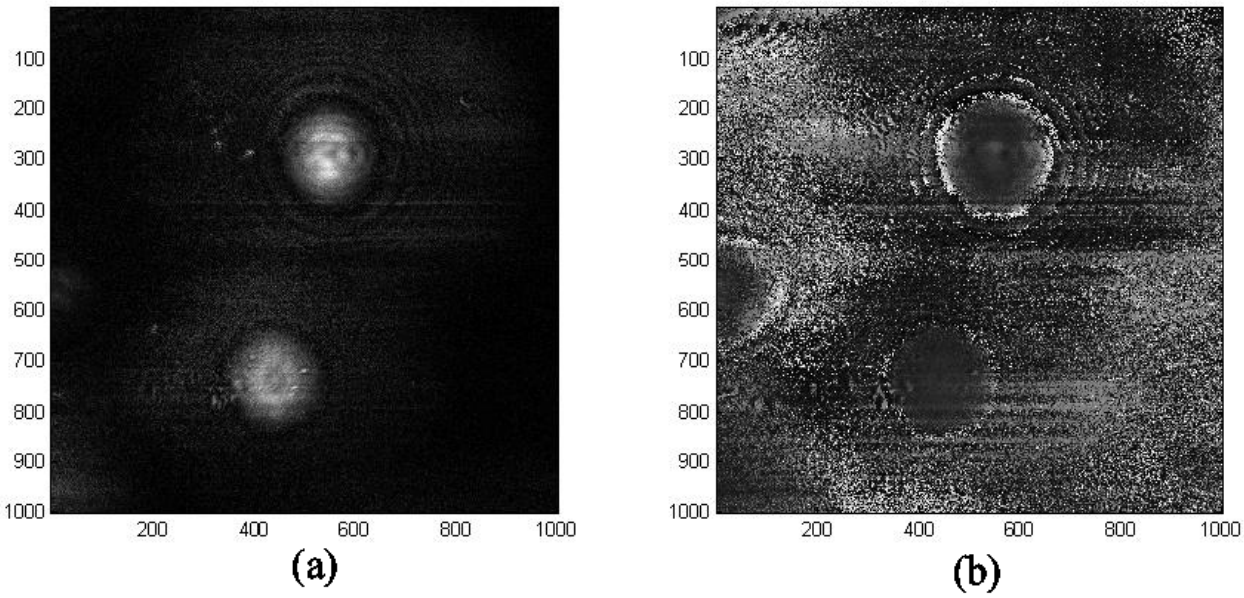

Fig. 3.
The magnitude and (b) The phase of the final hologram.

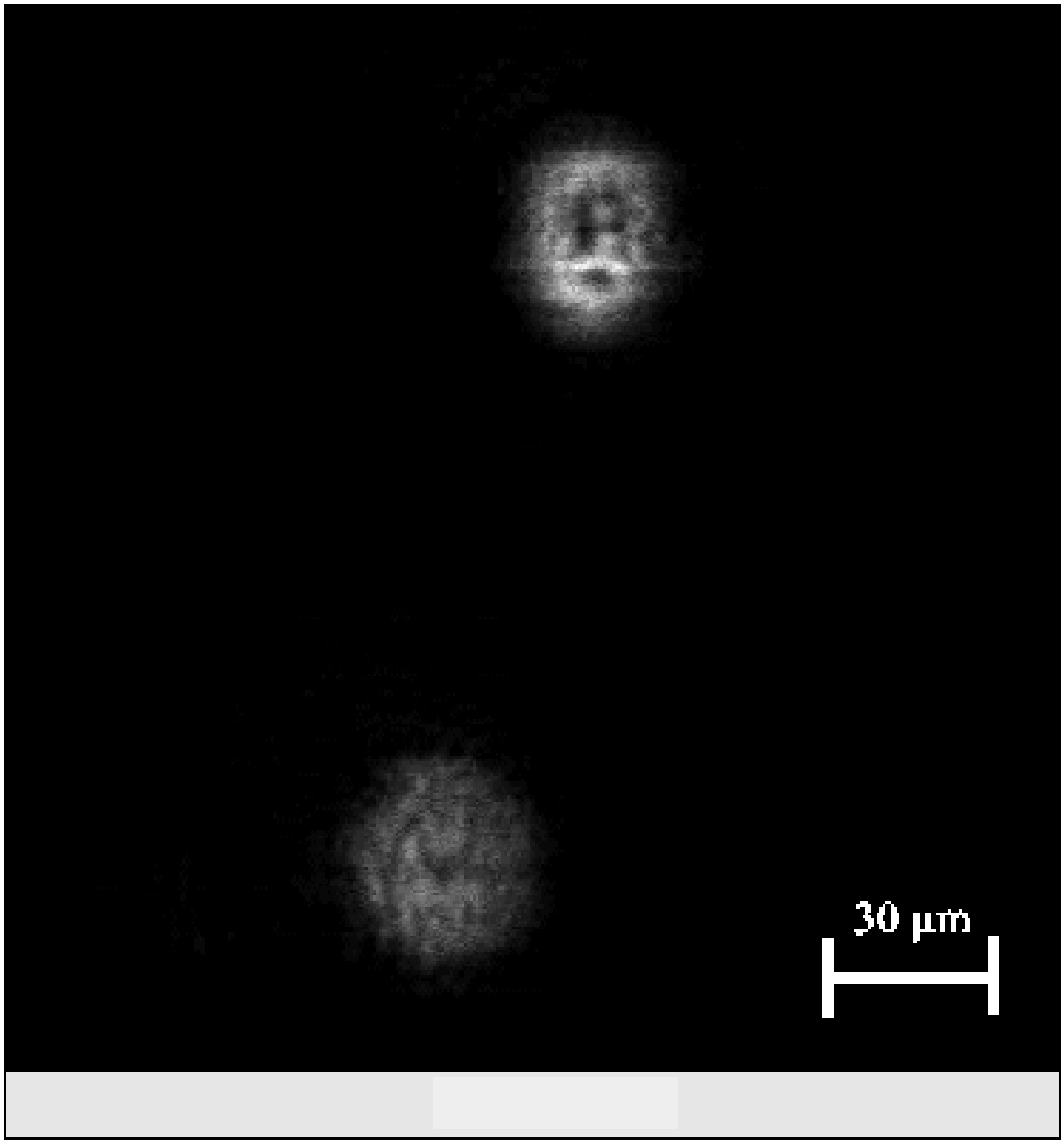

Fig. 4.
Movie of the image reconstruction along the light propagation axis.